UNITED JOURNAL OF CHEMISTRY
An International Open Free Access, Peer Reviewed Research Journal
www.unitedjchem.org

ISSN: 2581-7760
CODEN: UJCHEG
2018, Vol. 01, No.(1):
Pg. 82-91

The Method of Preparation of Ni Nanopowders with Controlled Mean Specific Surface and Pyrophoricity

MICHAIL I. ALYMOV[1], NICKOLAI M. RUBTSOV*[1], BORIS S. SEPLYARSKII[1], VICTOR A. ZELENSKY[1], ALEXEY B. ANKUDINOV[2]

[1]Institute of Structural Macrokinetics and Material Sciences (ISMAN) of Russian Academy of Sciences, Acad. Osyp'an street 8, 142432 Chernogolovka, Russia.
[2]Institute of Metallurgy and Material Science Russian Academy of Sciences, 119991 Leninsky avenue, 49, Moscow, Russian Federation.
Corresponding author E-mail: nmrubtss@mail.ru

(Received: August 22, 2018; Accepted: September 25, 2018)

ABSTRACT

It is revealed that nickel nanopowder synthetized by thermal decomposition of nickel formate in hydrogen flow is pyrophoric at 200C; the nanopowder is not pyrophoric in dehumidified air at temperatures lower than – 30C. However, its surface reacts with the air; the process stabilizes nickel nanopowder at room temperature. It is shown that nickel nanopowder obtained from nickel formate in argon at 2090C and the subsequent processing of the nanopowder in hydrogen flow during the specified time interval allows controlling the level of pyrophoricity and the mean specific surface of the nanopowder.

Keywords: nickel nanopowder, passivation, pyrophoricity, nickel formate, subzero temperatures.

INTRODUCTION

Nanotechnology incorporates methods of obtaining of materials with both nanometer structure sizes and nanometer- size objects. The transition to a nanodimensional state in which the characteristic geometrical sizes of structure of a substance are proportionate with the certain characteristic scale of some physical phenomenon, causes marked changes in the characteristics of the substance as compared to bulk one.

The nanopowders of metals are pyrophoric, i.e. they are capable of self-ignite in air because of high chemical activity and a large specific surface. To make safe a further processing of nanopowders to products, the powders are protected (passivated). The passivation means the synthesis of a protective thin oxide film on a surface of nanoparticles, which allows avoiding self-ignition of metallic nanopowders. There have been no scientifically grounded methods of passivation of metallic nanopowders.

Recently, many investigations were focused on the synthesis of uniform nanosized nickel nanoparticles because of their specific properties and eventual applications in a variety of fields namely electronics1-3, and biomedicine4. As compared to noble metals, nickel nanoparticles have been less investigated in catalysis, although they are extensively used both in the growth of carbon nanotubes5 and in a variety of organic reactions as well6.Obtaining of nickel nanoparticles in the zero valent state is not trivial, since they readily undergo oxidation, consequently affecting their catalytic efficiency7. Nickel nanoparticles are mainly synthesized by the chemical reduction of a nickel (II) salt, with the polyol process8, hydrazine9 or sodium borohydride10. In the processes, the presence of some protective agent is necessary to prevent particle agglomeration and oxidation. Futhermore, there are a considerable number of publications dealing with the control of the metal particle size. However, regularly the synthesized metal nanoparticles are only characterized but not utilized in any applications. Thus, conservation methods for the nanoparticles of controlled size are essential to be developed.

Therefore, in spite of its high potential for different applications, there is limited knowledge about the properties of nickel nanopowders such as size and pyrophoricity. It is known that the nanopowders of metals, in particular, nickel nanopowders, are pyrophoric immediately after synthesis. They self-ignite in air because of high chemical activity and a large specific surface. To make safe a further processing of nanopowders to products, the powders can be protected (passivated). The passivation means the synthesis of a protective thin oxide film on the surface of nanoparticles, which allows avoiding their self-ignition.

In11, the reliable method of stabilization of Ni nanoparticles synthesized from Ni formate in H2 flow by an option of the method of chemical metallurgy and further passivation in argon + 3% air flow within 3 ÷ 10 minutes has been suggested. The finger-like mode of the combustion of non passivated Ni nanopowders in air without external flows directed along the surface has been revealed. It has been shown that the time of completion of passivation in almost identical with the time of the beginning of cooling down of the nanopowder sample during passivation. The method of X-ray phase analysis showed that 2 mm thick samples of Ni nanopowder passivated in 3% air + Ar flow for more than 5 min contain only metallic Ni. The nanoparticles form crystallites with a size ~ 50 ÷110 nanometers. The BET specific surface area of the passivated Ni nanoparticles made up~ 5.2 ÷ 7.6 m2/g.

The work is aimed at the following facts. First, we found previously that at certain subzero temperature Fe nanopowder does not ignite in dehumidified air[12]; however, passivation with the air takes place and the nanopowder becomes stable in the air at room temperature. Second, we showed that thermal decomposition of Ni formate powder upon heating in Ar flow leads to formation of not pyrophoric Ni nanopowders.

The objective of the work is both to develop ideas12 to Ni nanopowders and to work out an original method of the synthesis of nanopowders allowing consciously control their size and pyrophoricity. This will ensure the demanded safety level of the processing of Ni nanopowders at maintaining their unique properties. The method is based on Ni nanoparticles passivation at subzero temperatures in dry air flow, in this case Ni nanoparticles will be produced by decomposition of Ni formate at 2090C upon heating first in Ar and then in H2 flow. The objective of the study was to examine certain properties of Ni nanoparticles synthesized by this method.

MATERIALS AND METHODS

Nickel nanopowders were synthesized as follows. The main stages of obtaining of Ni nanopowders are a synthesis of Ni formate by the reaction between nickel hydroxide with formic acid11. The synthesis of nickel hydroxide was performed using alkali treatment of nickel sulfate, sedimentation and drying of the hydroxide. Ni formate usually occurs as dihydrate. When it is heated, it loses water at ~ 140 °C ; then it begins to decompose at ~ 210 °C to give a finely divided Ni powder with evolution of a gas mixture composed mainly of carbon dioxide, hydrogen and water by the following reactions13:

$$Ni(HCOO)_2 \cdot 2H_2O \rightarrow Ni + 2CO_2 + H_2 + 2H_2O$$

$Ni(HCOO)_2 . 2H_2O \rightarrow Ni + CO + CO_2 + 3H_2O$

The reactor (Fig.1) with samples of Ni formate powder 1, 2, 3, 4 and 5 mm thick in the quartz trough was heated during 70 min at 209 °C in hydrogen or Ar flow; then it was cooled down to room temperature in argon flow.

For protection (passivation) of Ni nanopowder, which was carried out in the reactor, the sample was treated with the gas mixture 3 % air + argon at 200C.

The quartz trough, in which the sample was placed, was provided with a chromel - alumel thermocouple (0.15 mm) placed in the powder; the thermocouple did not contact the trough. If passivation was performed at temperatures lower than room one, the reactor was put inside an external bath of a cryostat HAAKE-Q (Germany) and cooled down to + 3 ÷ -10 °C in an argon flow with ethyl alcohol as a cooling agent. Upon reaching the necessary temperature Ar flow was replaced by a dehumidified air flow. To obtain dehumidified air, it was passed through a column of solid alkali (KOH) and then the coil of a flexible tubing placed in the internal bath of the cryostat[12]. The warming up of a sample indicated with the thermocouple after replacing flows pointed to the beginning of the reaction of Ni oxidation. The infrared camera Flir 60 (60 frames/s, resolution 320x240 pix, sensitivity interval 8 – 14 μm) was used for monitoring of the dynamics of change in temperature of a sample in the processes of passivation and combustion.

If an ignition occurred, finger-like propagating waves of reaction originating from initial centers were observed (initial temperature is more than 20C, Fig. 2a. If there was no ignition in 10 min, the air flow was replaced with the Ar flow and the reactor was heated up to room temperature. Then the quartz trough with the sample was extracted from the reactor.

X-ray Diffray-401 diffractometer (Russia) with a coordinate-sensitive detector was used to investigate phase structure of the samples. AES spectra were obtained with an Auger spectrometer JEOL JAMP-9500F (Japan) with 3 nm resolution in SEI (secondary emission image) mode (at 25 kV, 10Pa). The diameter of an electronic probe was 8 nm (at 25 kV, 1Pa), the accelerating voltage of 0,5 - 30 kV. The device was equipped with an electrostatic hemispherical analyzer and multichannel ionic gun with the energy of ions from 0.01 to 4 keV. The analyzer Sorbi-M was used for measurement of the mean values of specific surface by BET method. The microstructure of the powders was examined using field emission ultra-high resolution scanning electron microscope Zeiss Ultra Plus (Germany) investigation equipped with an X-ray microanalysis console INCA 350 Oxford Instruments.

RESULTS AND DISCUSSION

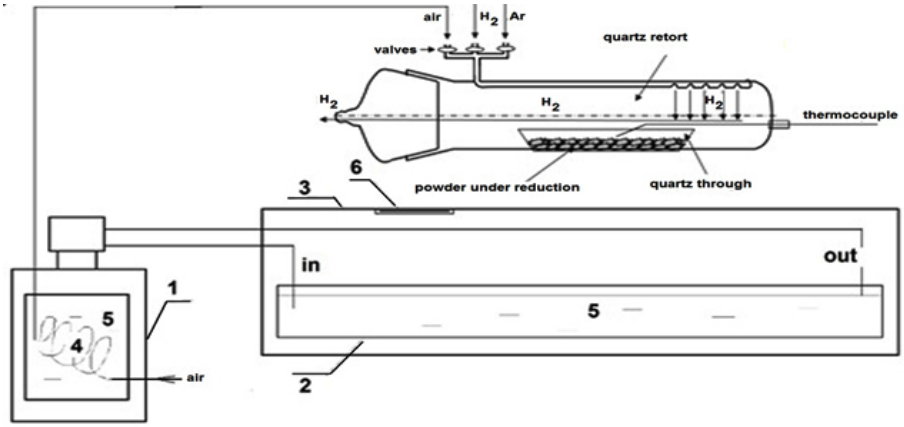

Fig.1: a) –experimental installation, 1 – cryostat HAAKE-Q, 2 – external cooling bath, 3- thermal isolating cover, 4 – a coil for air dehumidifying, 5 – ethyl alcohol, 6 – an opening for filming

Frame sequences of IR video filming of interaction of Ni nanopowders with dry air flow at initial temperatures 2oC (a) and – 3oC (b) are presented in Fig.2. The nanopowders were obtained from Ni formate in H2 flow at 2090C for 70 min.

In the visual analysis of data of infrared video filming it is necessary to consider the features of image processing with the Flir 60 infrared camera: the area with the maximum value of temperature of time has at the given moment identical brightness for all shots irrespective of the actual value of temperature. Real values of the maximum and minimum temperature at the moment are shown at the left border of each shot.

As is clearly seen in Fig.2a (shots 1, 2) on the first stage of ignition initial centers occur against the background of a warming up of the whole sample. Then the finger-like propagating reaction waves originates from the hottest initial centers (shots 4-6). At -30C, as is seen in Fig. 2b, the spontaneous reaction of oxidation of Ni nanopowder with dry air occurs together with a warming up of the sample. However, as compared to Fig.2a, the oxidation accompanied by a small warming-up occurs almost simultaneously across the surface of the sample at lesser temperatures and without the pronounced combustion front. This means that the critical conditions of the local ignition, leading to flame front propagation are not implemented [14-16]. Thus, combustion modes at 2oC and - 3oC differ qualitatively. It should be pointed out that performing the passivation at low temperatures not only opens an opportunity to use the dry cooled air as the passivating agent, but (as it is shown below) provides both the reduction of the mean size of nickel nanoparticles after passivation and reduction of thickness of protective oxide film on nickel nanoparticles.

Typical dependencies of sample heating during passivation at different initial temperatures on time are shown in Fig.3.

As is seen in the Figure, the less initial temperature is the less a warming up is; in addition,

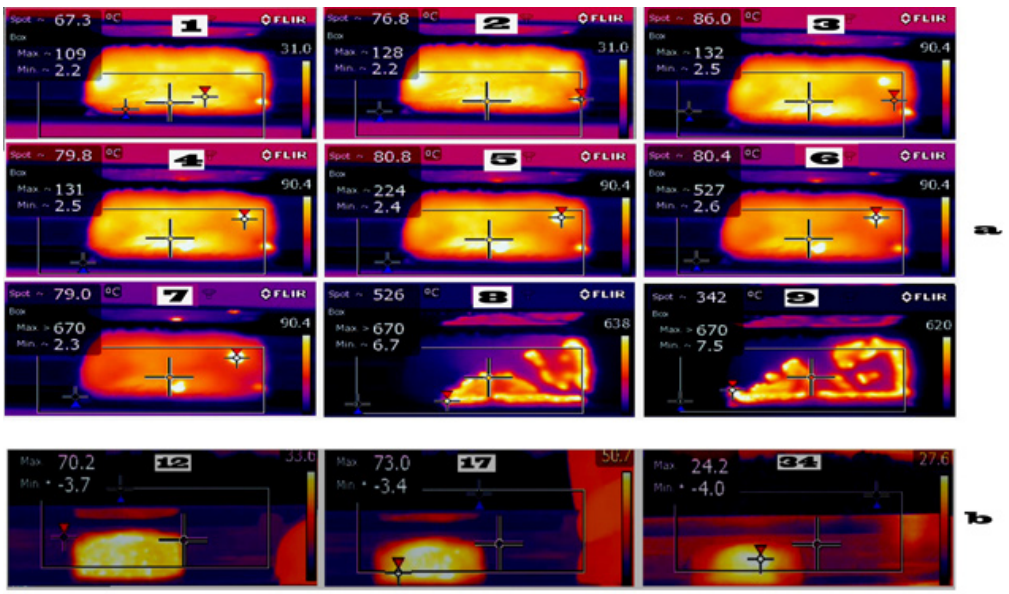

Fig.2: Frame sequences of IR video filming of the behavior of Ni nanopowders in the air at initial temperatures 2oC (a) and – 3oC (b). A number of a frame is the time in seconds from the moment of replacement of Ar flow by a flow of the dry cooled air. A bigger cross indicates the current temperature in the point, a smaller cross marked red automatically indicates the point, in which maximum temperature is achieved; a smaller cross marked blue indicates the point, in which minimum temperature is achieved over the rectangle in a frame.

at low initial temperature – 3oC the frontal mode of chemical transformation is missing. Small warming up values at T0 = – 8oC are also due to the warming up in the reaction of Ni oxidation accompanied by the emergence of a thin protective oxide film on the surface of Ni nanoparticles. The data obtained demonstrate that critical conditions of thermal ignition take place, which are resulting from the change of a ratio between thermal emission and heat losses14-16 for the samples of nickel nanopowder, just as for those of iron nanopowder12. Thus, theoretical approaches of the classical macroscopic theory of thermal explosion can be applicable for the description of the phenomena of ignition of macroscopic objects of nanoparticles; it appears to be a general principle.

It is known17 that the activation energy of oxidation of pyrophoric nickel powder by oxygen makes 3100±300 cal/mole that is typical of surface processes18. We note that activation energy of oxidation of Fe nanopowder makes ~ 7500 cal/mole12. This value of activation energy is in a good consent with that of oxidation of the pyrophoric Fe powder (4900±700 cal/mole) determined in17. Such consent is an additional argument in favor of the surface mechanism of oxidation of nanopowders of metals.

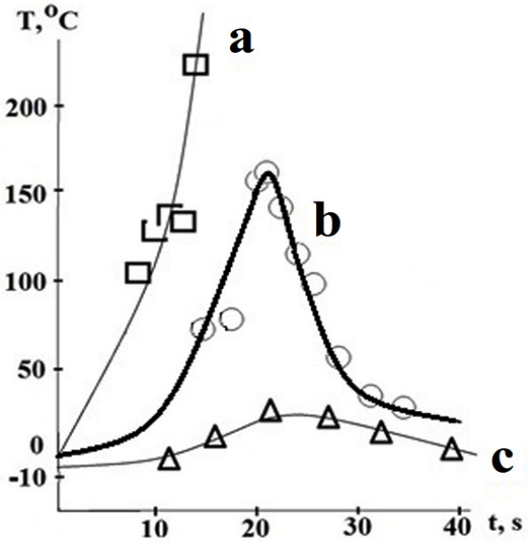

Fig. 3: Time dependencies of maximum warming up of the sample during passivation. Curves a) and b) correspond to 2oC and -3oC respectively: frame sequences a) and b) in Fig.2; the curve c) at -80C the temperature is measured with a thermocouple.

X-ray phase analysis showed that nonpassivated samples after combustion (T0 ≥ 20C) in air contain nickel oxides and the noticeable amount of metallic nickel, whereas the sample of nanopowder passivated in the dehumidified air for more 10 min at T0 < -3oC contains only metallic nickel. As the X-ray method for the samples processed at T0 < -3oC detects only nickel and nickel oxides are not detected at all, an oxide layer is either amorphous or quite thin4.

If we assume that the time of complete passivation corresponds to the cooling the sample to the room temperature, then, as is seen in Fig. 3c, the passivation process at T0 < -80C comes to an end in 1 min after the start of air supply. It allowed limiting passivation time to five minutes. In that experiment, in 5 min, in accordance with the reading of the thermocouple, the air flow was replaced with the Ar flow. Then the reactor was heated up to room temperature. The X-ray method for the sample processed at – 8oC and treated in the dry air for 5 min, detected only nickel.

Auger measurements were used for estimating the thickness of the passivating oxide film. Fig. 4a shows Auger spectrum of the protected surface of Ni nanopowder. It shows that the passivated particles contain Ni and O atoms along with usually detectable carbon (C) impurity. The secondary emission image (SEI) of passivated at 200C Ni nanoparticles recorded in H2 flow at 2090C for 70 min (passivation time is 10 min at 200C in 3% air + Ar flow), and SEI image of Ni nanopowder recorded at -80C under similar conditions are presrnted in Fig 4b, 4c correspondingly. Notice that the values of atomic concentration are largely qualitative as the probing beam in the position of the analysis can touch the particles lying below. This does not take place in the analysis of thin films.

It is seen that Ni particles exist in contact with each other, forming agglomerates; as one can see in the Figures, the average size of nickel nanoparticles, protected at -80C is noticeably less than that for those passivated at 200C (~100 nm11). This agrees with the fact that the processed

of agglomeration and coalescence of nickel nanoparticles slow down at lower temperatures (see below). The results of AES depth profile analysis for three points on the samples 4b and 4c are shown in Fig. 4b1 (200C) and 4c1 (-80C) correspondingly. As is seen, the concentration value of oxygen atoms for Ni nanoparticles, protected at 200C becomes close to zero at a depth of > 8nm; the concentration value of oxygen atoms for Ni nanoparticles, passivated at -80C becomes close to zero at a depth < 6 nm. Thus, the average thickness of the protecting oxide film on a nickel nanoparticle is smaller than for that obtained at -80C. The average thickness of the protecting oxide film for the particles obtained at -80C can be assessed as ~ 5 nm taking into account the mentioned fact that the probing beam touches the layers lying below.

In addition to Auger investigation, electronic microscopy was used. In Fig. 5, the photographs obtained by scanning electron microscope investigation of the protected nickel nanopowders are presented. The nanopowder passivated at 200C for 10 min is presented in Fig.5a, and nanopowder passivated in the stream of dehumidified air for 5 min at -80C is shown in the Fig 5b. Such noticeable distinction between the sizes of the nanoparticles passivated at 200C and - 80C is generally due to the fact that with an increase in the temperature of the environment, the velocities of diffusive migration and coalescence processes in the adsorption layer considerably increase10.

In the next series of experiments, it was found that the heating of samples of Ni formate powder during 70 min at 209 °C in Ar flow does not provide the formation of pyrophoric Ni, however Ni nanopowders synthetized in Ar flow have the smaller size than those obtained in H2 flow (Fig.5c). In Fig. 5, the photographs of nickel nanopowders synthesized in H2 flow with further passivation (Fig.5a) and Ni nanopowders obtained in Ar flow (Fig.5c) are

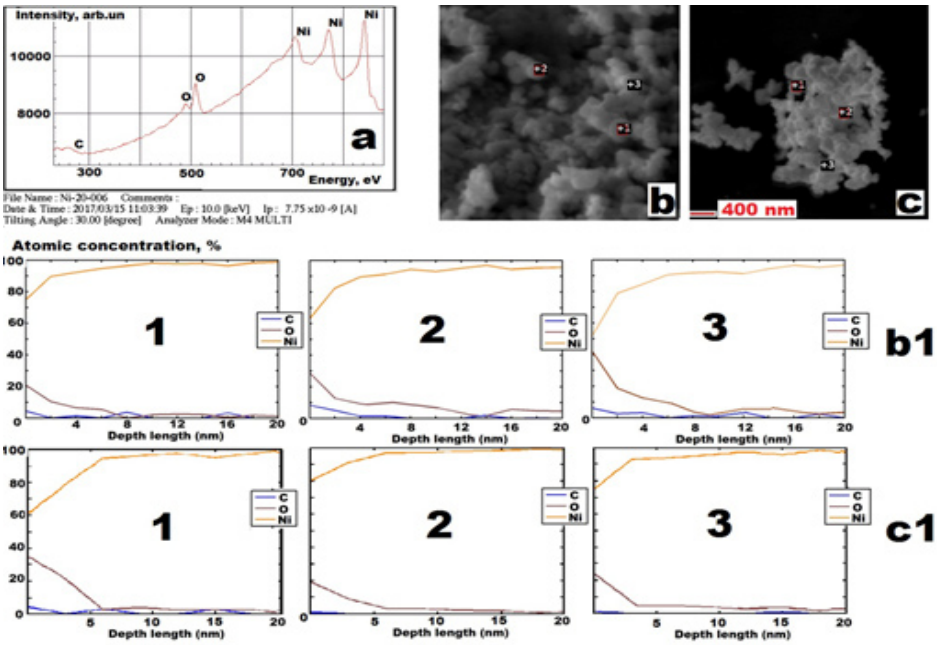

Fig. 4: a) Auger spectrum of Ni nanopowder,
b) SEI image of Ni nanopowder passivated at 20^{0}C;
c) SEI image of Ni nanopowder passivated at -8^{0}C ;
b1) AES depth profile of the subsurface composition of nickel nanopowder after 10 min of treatment with the 3% air + Ar flow at 20^{0}C at three points;
c1) AES depth profile of the subsurface composition of nickel nanopowder obtained at -8^{0}C at three points (5 min of treatment with the 3% air + Ar flow);
The image, spectrum and profiles were obtained at 20^{0}C.

presented. As is seen in the Figure, Ni particles exist in contact with each other, forming agglomerates; the average size of Ni nanoparticles, obtained in Ar flow is markedly smaller than that for those synthesized in H2 flow.

The cause of pyrophoricity of Ni nanoparticles obtained in H_2 flow is that the processing of Ni formate in H_2 flow instead of Ar prevents either NiO formation (in this case NiO is reduced to Ni) or CO interaction with active Ni as a result of the process $Ni(HCOO)2.2H_2O \rightarrow Ni + CO + CO_2 + 3H_2O$ (CO reacts with H2 on active Ni surface and suppresses Ni activity) 13.

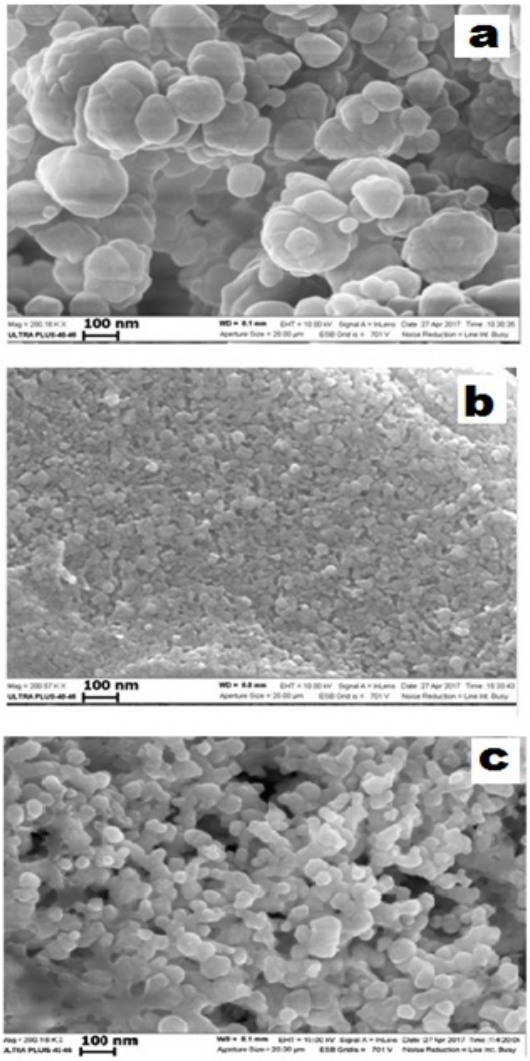

Fig. 5: Photos of the nickel nanopowders a) passivated at 20^{0}C for 10 min in the flow 3% air + Ar ; b) passivated at -8^{0}C for 5 min in the flow of dehumidified air (right).c) 70 min in Ar flow without passivation. Sample thickness is 2 mm.

In Fig.6, the dependencies of BET specific surface area of Ni nanoparticles on the sample thickness are presented. Thick empty circles refer to Ni nanoparticles synthetized in Ar flow. Thin empty circles refer to protected Ni nanoparticles obtained in H2 flow and then treated for 10 min with argon + 3% air flow. For instance, for Fig.6, formula evaluation d = 6/(s) for the 3mm thick sample obtained in Ar stream with s = 22.0 m2/g gives the value of an average nanoparticle diameter d = 30 nm (s – specific surface area, r= 8.902 g/cm^3 is the density of Ni) and for the 3mm thick sample obtained in H2 flow with s = 7.9 m2/g gives the value of an average nanoparticle diameter d = 85 nm.

A square - Ni nanopowder from Ni formate treated for 70 min in Ar, 10 min in H2 flow at 2090C (the sample is not pyrophoric).

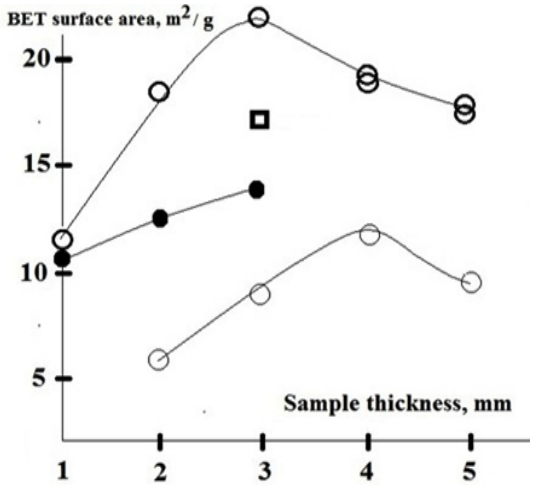

Fig. 6: Dependencies of BET specific surface area of Ni nanoparticles on the sample thickness. Thick empty circles – Ni nanopowder from Ni formate treated for 70 min in Ar flow at 209^{0}C. Thin empty circles - Ni nanopowder from Ni formate treated for 70 min H2 flow at 209^{0}C, 10 min passivation in argon + 3% air flow.

Filled circles - Ni nanopowder from Ni formate treated for 70 min in Ar, 10 min in H2 flow at 2090C, 15 min treatment in argon + 3% air flow. The curves were processed by means of the program package Statistica 9 (Statsoft).

Let's turn our attention to the dependence of the values of specific surface of Ni nanoparticles on the gas composition. Filled circles in Fig.6 refer to Ni nanoparticles obtained by treatment for 70 min in Ar then for 10 min in H2 flow and for 15 min passivation in argon + 3% air flow. Square refers to the synthesis for 70 min in Ar and 10 min in H2 flow without passivation. The passivation was not performed because the 3 mm thick sample under these conditions is warming up, but it does not burn (see Fig.7a). As is seen in Fig.6, the values of the average specific surface of the particles and correspondingly the average sizes of the particles lie between those obtained in the only Ar flow and in the only H_2 flow. Thus, one can assume that obtaining of Ni nanoparticles in Ar and their further treatment with H_2 for different time intervals will provide both controlling the mean specific surface of the nanoparticles and changing the level of pyrophoricity of the nanopowder. Notice that the dependence of BET specific surface area of Ni nanoparticles synthetized in Ar flow on the sample thickness has a maximum at 3÷4 mm. Thus, further the behavior of samples of 1, 2, 3 mm thickness was investigated.

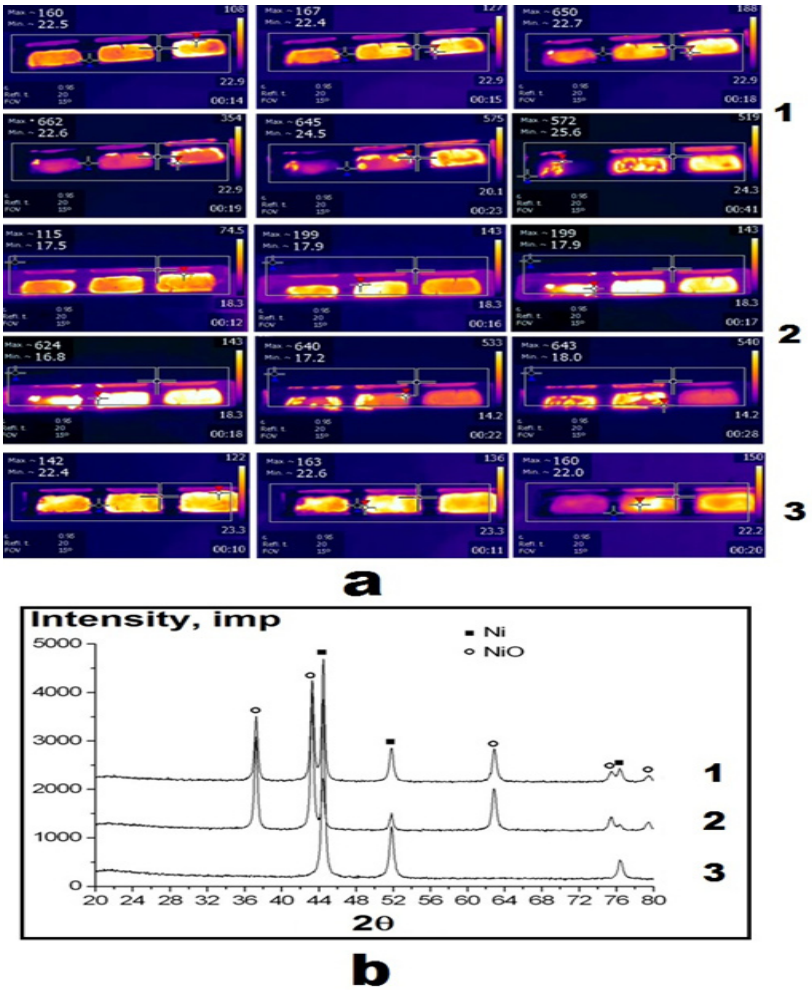

Fig. 7: a) Typical frame sequences of IR cinematography of Ni nanopowders. 20°C. 60 frames per second.

We have found that the nanoparticles obtained in Ar stream become pyrophoric under subsequent H2 treatment, because the pyrophoricity of the nanopowder depends both on the time interval of H2 processing and on the sample thickness. This dependence is revealed rather clearly in Fig. 7a. In Fig.7a, typical sequences of frames of simultaneous IR cinematography of behavior of nickel nanopowder in air (on each frame sequence from left to right: the samples of 1, 2, 3 mm thickness) are shown. In the bottom of each frame to the right, the time (s) after extraction of the nanopowder sample from the reactor is presented. Fig. 7a (1) presents combustion of Ni nanopowder samples of different thickness obtained by processing of Ni formate for 70 min in Ar and then for 30 min in H2 flow. As is seen in the Figure, the three samples burn in the air; the 3 mm thick sample ignites first. Fig 7a (2) shows combustion of Ni nanopowder obtained by treatment of Ni formate for 70 min in Ar and then for 10 min in H2 flow. As is seen, the sample 3 mm does not ignite at all; the sample 2 mm thick is ignited first. Finally, all the samples synthetized for 70 min in Ar flow without additional treatment in H2 flow do not burn altogether (Fig.7a (3)).

1. Combustion of Ni nanoparticles in the air (on each frame from left to right: the samples of 1, 2, 3 mm thickness). Ni formate treated for 70 min in Ar, 30 min in H2 flow at 2090C.
2. Combustion of Ni nanoparticles in the air (on each frame from left to right: the samples of 1, 2, 3 mm thickness). Ni formate treated for 70 min in Ar, 10 min in H2 flow at 2090C.

.. Warming-up of Ni nanopowder in the air (on each frame from left to right: the samples of 1, 2, 3 mm thickness). Ni formate treated for 70 min in Ar flow at 2090C. In the bottom of each frame, to the right the time (s) after extraction of the trough with nanopowder from the reactor is shown.

b) X-ray phase analysis of Ni nanopowders. The data refer to Fig. 7a (2).

1. Sample thickness 1 mm (Ni formate treated for 70 min in Ar and then 10 min in H2 no passivation, burnt);
2. Sample thickness 2 mm (Ni formate treated for 70 min in Ar and then 10 min in H2 no passivation, burnt);
3. Sample thickness 3 mm (Ni formate treated for 70 min in Ar and then 10 min in H2 no passivation, unburnt).

X-ray phase analysis of Ni nanopowder samples corresponding to Fig. 7a (2) is shown in Fig.7b. The results presented in the Figure support the conclusions on the features of interaction of the samples of different thickness with air after two-stage synthesis. The results presented in Fig.7b for different thicknesses of samples under the similar conditions of the synthesis indicate partial oxidation of the samples 1-2 and the lack of oxidation of the sample 3. As is shown in Fig. 7b, chemical transformation in the samples 1, 2 occurs incompletely; the burnt samples contain metallic Ni. Probably, this is caused by a finger-like (Fig.7a) character of combustion.
Notice that Ni nanoparticles of controlled average size obtained in Ar and further treated with H2 can be than passivated (10 min in 3% air + argon flow under our conditions) for conservation.

CONCLUSIONS

It is experimentally revealed that at the temperature lower than -30C Ni nanoparticles do not burn in dry air; however, passivation takes place; the process stabilizes nanoparticles at room temperature. It is shown that the samples of nickel nanoparticles passivated in dehumidified air contain only nickel.

With scanning electronic microscopy and AES methods, it is shown that passivation at the temperature lower than -30C prevents agglomeration and coalescense of Ni nanoparticles, therefore, the mean size of nanoparticles after passivation at - 80C is smaller than for those passivated at 200C.

It is experimentally shown that the heating of samples of Ni formate powder during 70 min at 209 °C in Ar flow does not lead to occurrence of pyrophoric Ni, however under these conditions the nanopowders have the minimum average size (30 nm).

The method of obtaining of Ni nanoparticles in Ar from Ni formate and further treatment of the nanoparticles with H2 for different time intervals allows both controlling the average size of the

nanoparticles and changing the level of pyrophoricity of the nanopowder.

It is shown that theoretical approaches of the classical macroscopic theory of thermal explosion can be applicable for the description of the phenomena of ignition of macroscopic objects of nanoparticles.

Funding

This work was supported by the Russian Science Foundation [grant number 16-13-00013].

REFERENCES

1. Tseng, W. ; Chen, C.; J. Mater. Sci., 2006, 41(4): 1213-1219.
2. Gubin, S.P. ; Koksharov, Y.A.; Khomutov, G.B.; Yurkov, G.Y.; Russ. Chem. Rev., 2005, 74 (6): 489-520.
3. Karmhag, R.; Tesfamichael, T.; Wackelgaard, E.; Nikalsson, G.; Nygren, M.; Sol. Energy, 2000, 68(4): 329-333.
4. Rodrıguez-Llamazares, S.; Merchan, J.; Olmedo, I.; Marambio, H.P.; Munoz, J.P. ; Jara, P.; Sturm, J.C.; Chornik, B.; Pena, O.; Yutronic, N.; Kogan, M.J.; J. Nanosci. Nanotechnol., 2008, 8(8): 3820-3827.
5. Geng, J. ; Johnson, B.F.G.; (Edmple s: Zhou, B.; Hermans, S. ; Somorjai G.A.), Nanotechnology in Catalysis, Berlin, Springer, 2004, 1: 159-189.
6. Polshettiwar, V.; Baruwati, B. ; Varma, R.S.; Green Chem., 2009, 11(1):127-131.
7. Song, P.; Wen, D.; Guo, Z.X.; Korakianitis, T.; Phys. Chem. Chem. Phys., 2008, 10(33): 5057-5065.
8. Bai, L.; Fan, J.; Cao, Y.; Yuan, F.; Zuo, A.; Tang, Q. ; J. Cryst. Growth, 2009, 311: 2474-2479.
9. Kim, K.H.; Lee, Y.B.; Lee, S.G.; Park, H.C.; Park, S.S.; Mater. Sci. Eng., 2004, A 381(1-2): 337-342.
10. Khanna, P.K.; More, P.V.; Jawalkar, J.P.; Bharate, B.G.; Mater. Lett., 2009, 63:1384–1386.
11. Alymov, M.I.; Rubtsov, N.M.; Seplyarskii, B.S.; Kochetkov, R.A.; Zelensky, V.A.; Ankudinov, A.B.; Mendeleev Comm., 2017, 27: 631-633.
12. Alymov, M.I.; Rubtsov, N.M.; Seplyarskii, B.S.;.Zelensky, V.A.; Ankudinov, A.B.; Mendeleev Comm., 2017, 27: 482-484.
13. Dean J. G.; Ind. Eng. Chem. Soc., 1952, 44: 985-993.
14. Zel'dovich, Ya.B., Selected works, Chemical Physics and Hydrodnamics, (Eds: Chariton Yu.A.), Moscow:; Ed. Nauka, 1984, (in Russian), 386.
15. Semenov, N.N.; On Some Problems of Chemical Kinetics and Reaction Ability, Moscow, Ed.Academy of Sciences USSR, 1958, (in Russian), 656.
16. Lewis, B.; Von Elbe, G.; Combustion, Explosions and Flame in Gases, New York, London.: Acad.Press, 1987, 566.
17. Repinski, S.M.; Introduction into chemical physics of the surface of solids, Novosibirsk, Ed. Nauka, Sibir publishing company, 1993, (in Russian), 265.
18. Gorrie, T.M.; Kopf, P.W.; Toby, S.; J. Phys. Chem., 1967, 71(12): 3842-3845.